Leptonic and semileptonic decays of mesons in the domain model of the QCD vacuum

Vladimir Voronin*

Joint Institute for Nuclear Research, 141980 Dubna, Moscow Region, Russia

(Received 16 April 2024; accepted 1 July 2024; published 26 July 2024)

The leptonic and semileptonic decays of mesons are investigated within the domain model of quantum chromodynamics (QCD) vacuum and hadronization. The domain model is the mean-field approach based on the statistical ensemble of almost everywhere homogeneous Abelian (anti-)self-dual gluon fields which reproduces main features of low-energy QCD and allows one to deduce a nonlocal effective meson action. Using this meson action, the leptonic decay constants, form factors and branching ratios of semileptonic decays are evaluated simultaneously with masses of mesons. The results are compared to experimental data or other approaches.

DOI: 10.1103/PhysRevD.110.014040

I. INTRODUCTION

The leptonic and semileptonic decays are most easily accessed processes, both theoretically and experimentally, which involve quark flavor transformation due to weak interaction. This makes them ideal for extracting the magnitudes of elements of Cabibbo-Kobayashi-Maskawa (CKM) matrix V from available experimental data. While the CKM matrix V concerns mixing of quarks, the experimental data are given for hadrons, which poses difficulties in extracting CKM elements, from the theoretical point of view. A multitude of methods can be employed in order to address this problem (see, e.g., [1–5] and references therein). Among them are lattice QCD, heavy quark effective theory, Dyson-Schwinger equations, sum rules and various quark models.

In this work, leptonic and semileptonic decays of mesons are investigated within the domain model of QCD vacuum and hadronization [6–12] which describes the composite nature of mesons with nonlocal meson-quark interaction. The domain model of QCD vacuum and hadronization consistently describes main features of low-energy QCD. The translation-invariant parts of gluon and quark propagators are entire analytical functions of complex momentum which can be interpreted as confinement of dynamical quarks [6]. It was shown in Ref. [13] that the vacuum ensemble also provides the area law for the Wilson loop, that is the confinement of static quarks. The vacuum also provides chiral symmetry breaking and resolution of $U_A(1)$ problem [8]. The mean-field model of hadronization in the presence of Abelian (anti-)self-dual vacuum gluon fields developed in Refs. [6,7,9] allows to deduce an effective meson action via hadronization of one-gluon exchange of quark currents. The resulting collective colorless excitations describe extended (non-pointlike) mesons. It was shown that masses of mesons in the model exhibit Regge character at large orbital and radial quantum numbers [6]. The model describes masses of light, heavy-light mesons and heavy quarkonia [7], leptonic decay constants of pseudoscalar mesons and electromagnetic transition constants of vector mesons [9], decay constants of vector mesons into a couple of pseudoscalar ones [10], electromagnetic transition form factors of pseudoscalar mesons [10], dipole polarizabilities of pseudoscalar mesons [14]. The model was also applied to the anomalous magnetic moment of muon, in particular to dominating contributions due to strong interactions [15]. The present work adds leptonic decay constants of vector mesons and semileptonic form factors to the list of phenomena investigated with the domain model of QCD vacuum and hadronization. See also Refs. [16,17] summarizing results concerning weak interactions of mesons which were obtained within a related nonlocal model.

The paper is organized as follows. Section II contains description of the model. The leptonic decays of mesons are considered in Sec. III, and semileptonic decays in Sec. IV. The results are summarized in Sec. V.

II. DESCRIPTION OF THE DOMAIN MODEL

The effective meson action of the domain model of QCD vacuum and hadronization [6–12] is given by the following formulas in Euclidean space-time

*Contact author: voronin@theor.jinr.ru

$$Z = \mathcal{N}\int D\phi_{\mathcal{Q}} \exp\left\{-\frac{\Lambda^2}{2}\frac{h_{\mathcal{Q}}^2}{g^2 C_{\mathcal{Q}}^2}\int d^4x \phi_{\mathcal{Q}}^2(x) - \sum_{k=2}^{\infty}\frac{1}{k}W_k[\phi]\right\}, \tag{1}$$

$$W_k[\phi] = \sum_{\mathcal{Q}_1\ldots\mathcal{Q}_k} h_{\mathcal{Q}_1}\ldots h_{\mathcal{Q}_k}\int d^4x_1 \ldots \int d^4x_k \Phi_{\mathcal{Q}_1}(x_1)\ldots\Phi_{\mathcal{Q}_k}(x_k)\Gamma^{(k)}_{\mathcal{Q}_1\ldots\mathcal{Q}_k}(x_1,\ldots,x_k),$$

$$\Phi_{\mathcal{Q}}(x) = \int \frac{d^4p}{(2\pi)^4} e^{ipx}\mathcal{O}_{\mathcal{Q}\mathcal{Q}'}(p)\tilde{\phi}_{\mathcal{Q}'}(p), \qquad C_{\mathcal{Q}} = C_J, \qquad C^2_{S/P} = 2C^2_{V/A} = \frac{1}{9}. \tag{2}$$

Here the index $\mathcal{Q} \equiv \{aJLn\}$ stands for all quantum number of a meson. Λ is the strength of background gluon field related to the condensate $\langle g^2F^2\rangle$. Auxiliary fields $\Phi_{\mathcal{Q}}$ introduced during hadronization are transformed into physical meson fields $\phi_{\mathcal{Q}}$ by an orthogonal matrix $\mathcal{O}_{\mathcal{Q}\mathcal{Q}'}$, so the quadratic term $W_2[\phi]$ in Eq. (2) becomes diagonal.

Inverting the quadratic part of the effective action, one finds corresponding propagators of meson fields $\phi_{\mathcal{Q}}$

$$D_{\mathcal{Q}}(p^2) = h_{\mathcal{Q}}^{-2}\left(\frac{\Lambda^2}{g^2C_{\mathcal{Q}}^2} + \tilde{\Gamma}^{(2)}_{\mathcal{Q}}(p^2)\right)^{-1}, \tag{3}$$

where $\tilde{\Gamma}^{(2)}_{\mathcal{Q}}$ is the two-point correlation function diagonalized with respect to all quantum numbers and g is strong coupling constant. The constants $h_{\mathcal{Q}}$ defined by the formula

$$1 = h_{\mathcal{Q}}^2\frac{d}{dp^2}\tilde{\Gamma}^{(2)}_{\mathcal{Q}}(p^2)\Big|_{p^2=-M^2_{\mathcal{Q}}}$$

provide that the residue at the pole of meson propagator (3) is equal to unity.

The general function $\Gamma^{(k)}_{\mathcal{Q}_1\ldots\mathcal{Q}_k}(x_1,\ldots,x_k)$ includes "connected" and "disconnected" terms correlated by background gluon field. For example, $\tilde{\Gamma}^{(2)}_{\mathcal{Q}\mathcal{Q}'}(p)$ is given by

$$\Gamma^{(2)}_{\mathcal{Q}_1\mathcal{Q}_2} = \overline{G^{(2)}_{\mathcal{Q}_1\mathcal{Q}_2}(x_1,x_2)} - \Xi_2(x_1-x_2)\overline{G^{(1)}_{\mathcal{Q}_1}G^{(1)}_{\mathcal{Q}_2}}. \tag{4}$$

Here Ξ is correlation function of the background field which characterizes the statistical ensemble of the almost everywhere homogeneous Abelian (anti-)self-dual fields. $G^{(k)}_{\mathcal{Q}_1\ldots\mathcal{Q}_k}$ are quark loops averaged over background field with measure $d\sigma_B$

$$\begin{aligned}\overline{G^{(k)}_{\mathcal{Q}_1\ldots\mathcal{Q}_k}(x_1,\ldots,x_k)} &= \int d\sigma_B \mathrm{Tr} V_{\mathcal{Q}_1}(x_1)S(x_1,x_2)\ldots V_{\mathcal{Q}_k}(x_k)S(x_k,x_1),\\ &\times \overline{G^{(l)}_{\mathcal{Q}_1\ldots\mathcal{Q}_l}(x_1,\ldots,x_l)G^{(k)}_{\mathcal{Q}_{l+1}\ldots\mathcal{Q}_{l+k}}(x_{l+1},\ldots,x_{l+k})}\\ &= \int d\sigma_B \mathrm{Tr}\{V_{\mathcal{Q}_1}(x_1)S(x_1,x_2)\ldots V_{\mathcal{Q}_k}(x_l)S(x_l,x_1)\}\\ &\times \mathrm{Tr}\{V_{\mathcal{Q}_{l+1}}(x_{l+1})S(x_{l+1},x_{l+2})\ldots V_{\mathcal{Q}_{l+k}}(x_{l+k})S(x_{l+k},x_{l+1})\}.\end{aligned} \tag{5}$$

Here $S(x,y)$ is a quark propagator in background gluon field, and $V_{\mathcal{Q}}$ is a nonlocal meson-quark vertex.

It is possible to find analytical expressions for propagators and vertices if one approximates the ensemble of almost everywhere homogeneous (anti-)self-dual Abelian background gluon field with just homogeneous field. The averaging over the ensemble is then implemented by averaging the quark loops (5) over configurations of homogeneous gluon field. These include self-dual and anti-self-dual fields with different directions in Euclidean and color spaces. The averaging over spatial directions can be found with the help of generating formula

$$\int d\sigma_B \exp(if_{\mu\nu}J_{\mu\nu}) = \frac{\sin\sqrt{2(J_{\mu\nu}J_{\mu\nu} \pm J_{\mu\nu}\tilde{J}_{\mu\nu})}}{\sqrt{2(J_{\mu\nu}J_{\mu\nu} \pm J_{\mu\nu}\tilde{J}_{\mu\nu})}}, \tag{6}$$

where $J_{\mu\nu}$ is an arbitrary antisymmetric tensor. Tensor $f_{\mu\nu}$ stands for an Abelian (anti-)self-dual background field with strength Λ:

$$\hat{B}_\mu = -\frac{1}{2}\hat{n}B_{\mu\nu}x_\nu, \qquad \hat{n} = t^3\cos\xi + t^8\sin\xi,$$
$$\tilde{B}_{\mu\nu} = \frac{1}{2}\epsilon_{\mu\nu\alpha\beta}B_{\alpha\beta} = \pm B_{\mu\nu}, \qquad \hat{B}_{\rho\mu}\hat{B}_{\rho\nu} = 4\upsilon^2\Lambda^4\delta_{\mu\nu},$$
$$f_{\alpha\beta} = \frac{\hat{n}}{2\upsilon\Lambda^2}B_{\alpha\beta}, \qquad \upsilon = \mathrm{diag}\left(\frac{1}{6},\frac{1}{6},\frac{1}{3}\right), \qquad f_{\mu\alpha}f_{\nu\alpha} = \delta_{\mu\nu}. \tag{7}$$

The upper sign in "±" should be taken for self-dual field, and the lower for anti-self-dual field.

Nonlocal vertices $V^{aJln}_{\mu_1\ldots\mu_l}$ are given by the following formulas:

$$V^{aJln}_{\mu_1\ldots\mu_l} = \mathcal{C}_{ln}\mathcal{M}^a\Gamma^J F_{nl}\left(\frac{\overleftrightarrow{\mathcal{D}}^2(x)}{\Lambda^2}\right)T^{(l)}_{\mu_1\ldots\mu_l}\left(\frac{1}{i}\frac{\overleftrightarrow{\mathcal{D}}(x)}{\Lambda}\right),$$
$$\mathcal{C}^2_{ln} = \frac{l+1}{2^l n!(n+l)!}, \qquad F_{nl}(s) = s^n\int_0^1 dt t^{n+l}\exp(st),$$
$$\overleftrightarrow{\mathcal{D}}^{ff'}_\mu = \xi_f\overleftarrow{\mathcal{D}}_\mu - \xi_{f'}\vec{\mathcal{D}}_\mu, \qquad \overleftarrow{\mathcal{D}}_\mu(x) = \overleftarrow{\partial}_\mu + i\hat{B}_\mu(x), \qquad \vec{\mathcal{D}}_\mu(x) = \vec{\partial}_\mu - i\hat{B}_\mu(x),$$
$$\xi_f = \frac{m_{f'}}{m_f + m_{f'}}, \qquad \xi_{f'} = \frac{m_f}{m_f + m_{f'}}. \tag{8}$$

Here $\mathcal{M}^a$ is a flavor matrix for a given meson, Γ^J is a corresponding Dirac matrix

$$\Gamma^S = 1, \qquad \Gamma^P = i\gamma_5, \qquad \Gamma^V_\mu = \gamma_\mu, \qquad \Gamma^A_\mu = \gamma_5\gamma_\mu,$$

constants $\xi_f, \xi_{f'}$ provide that x is a center of mass for quarks with flavors f and f', and n, l are radial and orbital quantum numbers, correspondingly. Function F_{nl} is defined by the propagator of gluons charged with respect to the background field, $T^{(l)}$ are irreducible tensors of four-dimensional rotation group. Propagator of the quark with mass m_f in the presence of the homogeneous Abelian (anti-)self-dual gluon field has the form

$$S_f(x,y) = \exp\left(-\frac{i}{2}\hat{n}x_\mu B_{\mu\nu}y_\nu\right)H_f(x-y),$$
$$\tilde{H}_f(p) = \frac{1}{2\upsilon\Lambda^2}\int_0^1 ds e^{(-p^2/2\upsilon\Lambda^2)s}\left(\frac{1-s}{1+s}\right)^{m_f^2/4\upsilon\Lambda^2} \times\left[p_\alpha\gamma_\alpha \pm is\gamma_5\gamma_\alpha f_{\alpha\beta}p_\beta + m_f\left(P_\pm + P_\mp\frac{1+s^2}{1-s^2} - \frac{i}{2}\gamma_\alpha f_{\alpha\beta}\gamma_\beta\frac{s}{1-s^2}\right)\right], \tag{9}$$

where anti-Hermitian representation of Dirac matrices is used, and "±" is the same as in formula (7), $P_\pm = (1\pm\gamma_5)/2$ is the chirality projector. The translation-invariant part H_f of the propagator is an analytical function in finite momentum plane which is interpreted as confinement.

A common way of extracting matrix V from experimental data is via matrix elements of quark currents. For example, leptonic decay constants of mesons are found from matrix element

$$\langle 0|\bar{q}'\gamma_\mu\gamma_5 q|H\rangle. \tag{10}$$

The formula (10) is known as impulse approximation which is often taken as a definition for corresponding amplitudes (see, e.g., review [2]). It is known that besides an ordinary boson-current interaction, in bound-state problems there is also an additional interaction with a gauge field which appears when the gauge invariance and current conservation are introduced in a consistent way [18–21]. The diagrammatical representation of these additional terms is shown in Fig. 1. When one includes photons and weak gauge bosons into the domain model, the interactions shown in Fig. 1 emerge, and their contributions to the amplitudes can be explicitly calculated, as well as those given by the impulse approximation.

Electromagnetic and weak interactions are introduced into the meson action in Eq. (2) in a gauge-invariant way with the prescription outlined in Ref. [18]. After this procedure and hadronization, the meson action includes local interactions contained in the Lagrangian of the

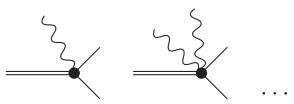

FIG. 1. Nonlocal meson-quark interaction with gauge bosons. The vertex with one gauge boson is of the first order in the gauge coupling constant, the vertex with two bosons is of the second order, and so on.

TABLE I. Values of parameters fitted to masses of π, ρ, K, K^*, D^0, B^0, and masses of other mesons evaluated with these parameters and used in calculations in the paper. $M_{\rm exp}$ for all mesons except B_c^* are taken from Ref. [23].

$m_{u/d}$, MeV	m_s, MeV	m_c, MeV	m_b, MeV	Λ, MeV	α_s
145	376	1715	5115	416	3.45

	π	K	ρ	K^*	D^0	B^0
$M = M_{\rm exp}$, MeV	139.57	493.67	775.26	891.66	1864.86	5279

	ω	ϕ	D^*	D_s	D_s^*	B^*	B_s	B_s^*	B_c	B_c^*
$M_{\rm exp}$, MeV	782	1019.46	2010.28	1968.35	2112.3	5325	5366.7	5415.4	6274.47	6328 [24]
M, MeV	775.26	1039	2088	1975	2235	5452	5373	5591	6312	6678

Standard Model and additional terms due to nonlocality (see Refs. [9,15]). The term relevant for the present paper yields a nonlocal meson-quark vertex with one charged gauge boson W^+,

$$V^{aJln;\mu}_{f_1f_2}(x;q) = -\frac{g}{\sqrt{2}}\int_0^1 d\tau \frac{1}{\tau}\frac{\partial}{\partial q_\mu} \times \left\{ P_R \begin{pmatrix} 0 & V^{\rm CKM} \\ 0 & 0 \end{pmatrix}_{f_1 f} V^{aJln}_{ff'}(\overleftrightarrow{\mathcal{D}}(x) - iq\tau\xi)\delta_{f'f_2} - \delta_{f_1 f} V^{aJln}_{ff'}(\overleftrightarrow{\mathcal{D}}(x) + iq\tau\xi') \begin{pmatrix} 0 & V^{\rm CKM} \\ 0 & 0 \end{pmatrix}_{f' f_2} P_L \right\}, \quad (11)$$

and its analog for W^-. Here $V^{\rm CKM}$ is CKM matrix, q is the momentum of W^+, $P_R = (1+\gamma_5)/2$ and $P_L = (1-\gamma_5)/2$ are chirality projectors, $g = e/\sin\theta_{\rm W}$, e is electric charge and $\theta_{\rm W}$ is weak mixing angle. Note that vertices (11) do not appear if one introduces weak interactions via Fermi four-fermion interaction.

Technically, the evaluation of one-loop diagrams reduces to Gaussian integrals over coordinates or momenta, averaging over background field using Eq. (6), analytical continuation to Minkowski space-time, and numerical integration over remaining proper times which appear in Eqs. (8), (9), and (11). The representation of vertex operator F_{nl} given in the Appendix helps reduce the complexity of Gaussian integrations within the computer algebra systems such as FORM [22] which was extensively used for evaluation of the amplitudes investigated in the present work.

The masses of mesons can be found from poles of corresponding propagators (1). The masses of π, ρ, K, K^*, D, B are used to extract the parameters of the model (see Ref. [9] for details): scale Λ related to gluon condensate $\langle g^2F^2\rangle$, quark masses and strong constant α_s. The parameters and evaluated masses are given in Table I. In practice, the matrix $O_{\mathcal{Q}\mathcal{Q}'}$ is truncated to some finite order, and in the present paper it is the matrix $O_{\mathcal{Q}\mathcal{Q}'} = O_{nn'}$ which mixes seven radial states. The masses of charmed and bottom quarks are extracted from D^0 and B^0 mesons instead of J/ψ and Υ in previous papers, e.g., [9]. This helps reduce the errors due to phase space of semileptonic decays which depends on masses of mesons rather sharply. The leptonic decay constants of pseudoscalar mesons are recalculated in Sec. III for consistency.

The energies of decays considered below are far less than the mass of the weak gauge boson $W^\pm$, so it is sufficient to approximate the exchange of gauge boson with Fermi constant G_F. The values of G_F and CKM matrix elements $V_{qq'}$ are taken from PDG [23].

III. LEPTONIC DECAYS OF MESONS

The amplitude of leptonic decays of pseudoscalar mesons can be parametrized as

$$A(H(p) \to \ell(k)\bar\nu_\ell(k')) = \frac{G_F}{\sqrt{2}} V_{qq'}\bar\ell\gamma_\mu(1-\gamma_5)\nu_\ell M_H^\mu = i\frac{G_F}{\sqrt{2}} V_{qq'}\bar\ell\gamma_\mu(1-\gamma_5)\nu_\ell f_H p^\mu \quad (12)$$

and for vector mesons as

$$A(H(p) \to \ell(k)\bar\nu_\ell(k')) = \frac{G_F}{\sqrt{2}} V_{qq'}\bar\ell\gamma_\mu(1-\gamma_5)\nu_\ell M_H^{\mu\nu}\vec{e}_\nu(p) = \frac{G_F}{\sqrt{2}} V_{qq'}\bar\ell\gamma_\mu(1-\gamma_5)\nu_\ell M f_H \vec{e}^\mu(p),$$

FIG. 2. Diagrams contributing to leptonic decay of mesons. The gray background denotes averaging over vacuum gluon field.

where $p^2 = M^2$, $k^2 = m^2$, $k'^2 = 0$. Here $V_{qq'}$ is the element of CKM matrix corresponding to a given decay, M is the mass of decaying meson, m is the mass of final lepton, and f_H is the constant which parametrizes hadronic part M_H of the corresponding amplitude. The diagrams contributing to the hadronic part of these decays are shown in Fig. 2. The gray background in the diagrams indicates that the background gluon field is taken into account nonperturbatively. The contribution of these diagrams for ground-state pseudoscalar mesons is

$$(2\pi)^4\delta^{(4)}(p-q)\frac{1}{2}V_{qq'}M_H^{\mu} = \sum_n O_{n0}^{aP}\left[\int d\sigma_B \int d^4x \int d^4y\, e^{ipx-iqy}(-1)\mathrm{Tr}V^{aP0n}(x)S(x,y)\gamma^{\mu}\frac{1-\gamma_5}{2}V^{\mathrm{CKM}}S(y,x) + \int d\sigma_B \int d^4x\, e^{ipx-iqx}(-1)\sum_n \mathrm{Tr}V^{aP0n;\mu}(x;-q)S(x,x)\right], \tag{13}$$

where $q = k + k'$ is momentum of virtual W boson, and a is the flavor index corresponding to the meson H. The trace is with respect to color, flavor and spinor indices. The matrix $O_{nn'}^{aJ}$ is found from location of the pole of propagator (3) for each meson. Analogous expression for the vector mesons is

$$(2\pi)^4\delta^{(4)}(p-q)\frac{1}{2}V_{qq'}M_H^{\mu\nu} = \sum_n O_{n0}^{aV}\left[\int d\sigma_B \int d^4x \int d^4y\, e^{ipx-iqy}(-1)\mathrm{Tr}V_{\nu}^{aV0n}(x)S(x,y)\gamma^{\mu}\frac{1-\gamma_5}{2}V^{\mathrm{CKM}}S(y,x) + \int d\sigma_B \int d^4x\, e^{ipx-iqx}(-1)\sum_n \mathrm{Tr}V_{\nu}^{aV0n;\mu}(x;-q)S(x,x)\right]. \tag{14}$$

The first term in these expressions corresponds to the matrix element of current given by formula

$$\langle 0|\bar{q}'\gamma_{\mu}(1-\gamma_5)q|H\rangle. \tag{15}$$

It can be noted that at large Euclidean momenta p the meson-quark vertex (8) behaves as $1/p^2$ if $l = 0$, and the vertex with gauge boson (11) behaves as $1/p^3$. Therefore the diagrams in Fig. 2 should logarithmically diverge. In order to regularize the divergences, one introduces a small positive shift ε into the lower boundary of integration with respect to t in Eqs. (8) and (11). Explicit calculation shows the sum of diagrams is finite after the regularization is removed, $\varepsilon \to 0$. Moreover, for pseudoscalar mesons each diagram in Fig. 2 is finite on their own, so it is possible to evaluate them separately. The results of calculations for pseudoscalar mesons are given in Table II, and for vector mesons in Table III.

TABLE II. Leptonic decay constants of pseudoscalar mesons compared to available data. The term in formula (13) corresponding to impulse approximation and matrix element (15) is given in column "impulse approximation," the column "full" includes all contributions given in Eq. (13).

		f_P, MeV, this work	
Meson	Decay constant f_P, MeV	Impulse approximation	Full
π	131.7 [23]	131.2	140.4
K	157.3 [23]	161.2	178.6
D	208.5 [23]	187.8	231.1
D_s	251.8 [23]	245.6	286.8
B	205.7 [23]	164.7	203
B_s	230.7 [25]	220.7	262.8
B_c	$427 \pm 6 \pm 2$ [26]	403.8	450.2

TABLE III. Leptonic decay constants of vector mesons. The calculated values are extracted from Eq. (14).

Meson	Decay constant f_V, MeV	f_V, MeV, this work
ρ	$208.5 \pm 5.5 \pm 0.9$ [27]	225.9
ϕ	241 ± 18 [28]	222.8
K^*	202.5 [23]	219
D^*	223.5 ± 8.7 [29]	174.3
D_s^*	268.8 ± 6.5 [29]	202.8
B^*	186.4 ± 7.1 [29]	133.4
B_s^*	223.1 ± 5.6 [29]	165.8
B_c^*	422 ± 13 [30]	299.8

IV. SEMILEPTONIC DECAYS OF MESONS

The amplitude of semileptonic decay $P \to P'\ell\bar{\nu}_\ell$ with a pseudoscalar meson in the final state

$$A(H(p) \to H'(p')\ell\bar{\nu}_\ell) = \frac{G_F}{\sqrt{2}} V_{qq'} \bar{\ell}\gamma_\mu(1-\gamma_5)\nu_\ell M^\mu_{HH'}$$

can be parametrized as

$$M^\mu_{HH'} = F_+(q^2)P^\mu + F_-(q^2)q^\mu, \tag{16}$$

where $P = p + p', q = p - p'$. The hadronic part of the amplitude $P \to V\ell\bar{\nu}_\ell$ with a vector meson in the final state

$$A(H(p) \to H'(p')\ell\bar{\nu}_\ell) = \vec{e}^{\,\dagger}_\alpha \frac{G_F}{\sqrt{2}} V_{qq'} \bar{\ell}\gamma_\mu(1-\gamma_5)\nu_\ell M^{\mu\alpha}_{HH'},$$

where $\vec{e}^{\,\dagger}_\alpha$ is polarization of vector meson, can be represented in the form suggested in Ref. [31]:

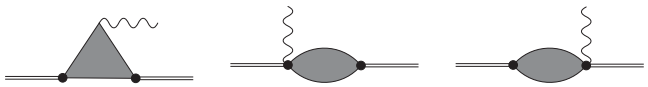

FIG. 3. Diagrams contributing to semileptonic decay.

$$\begin{aligned}
\vec{e}^{\,\dagger}_\alpha M^{\mu\alpha}_{HH'} &= -(M+M')\vec{e}^{\,\dagger}_\alpha g^{\mu\alpha} A_1(q^2) + \frac{\vec{e}^{\,\dagger}_\alpha q^\alpha}{M+M'} P^\mu A_2(q^2) \\
&\quad + 2M' \frac{\vec{e}^{\,\dagger}_\alpha q^\alpha}{q^2} q^\mu [A_3(q^2) - A_0(q^2)] \\
&\quad + \frac{2i\varepsilon^{\mu\alpha\rho\sigma}\vec{e}^{\,\dagger}_\alpha p'_\rho p_\sigma}{M+M'} V(q^2), \\
A_3(q^2) &= \frac{M+M'}{2M_2} A_1(q^2) - \frac{M-M'}{2M_2} A_2(q^2).
\end{aligned} \tag{17}$$

Here $A_0(0) = A_3(0)$.

The diagrams for semileptonic decay are shown in Fig. 3, and their contribution is given by the formula

$$\begin{aligned}
&(2\pi)^4\delta^{(4)}(p-p'-q)\frac{1}{2}V_{qq'}M^\mu_{HH'} \\
&= \sum_{nn'} O^{aP}_{n0} O^{a'P}_{n'0} \left[\int d\sigma_B \int d^4x \int d^4y \int d^4z\, e^{ipx-ip'y-iqz}(-1)\mathrm{Tr}V^{aP0n}(x)S(x,y)V^{a'P0n'}(y)S(y,z)\gamma^\mu \frac{1-\gamma_5}{2} V^{\mathrm{CKM}} S(z,x) \right. \\
&\quad + \int d\sigma_B \int d^4x \int d^4y\, e^{ipx-iqx-ip'y}(-1)\mathrm{Tr}V^{aP0n;\mu}(x;-q)S(x,y)V^{a'P0n'}(y)S(y,x) \\
&\quad \left. + \int d\sigma_B \int d^4x \int d^4y\, e^{ipx-ip'x-iqy}(-1)\mathrm{Tr}V^{aP0n}(x)S(x,y)V^{a'P0n';\mu}(y;-q)S(y,x) \right]
\end{aligned} \tag{18}$$

for final-state pseudoscalar mesons and

$$\begin{aligned}
&(2\pi)^4\delta^{(4)}(p-p'-q)\frac{1}{2}V_{qq'}M^{\mu\nu}_{HH'} \\
&= \sum_{nn'} O^{aP}_{n0} O^{a'V}_{n'0} \left[\int d\sigma_B \int d^4x \int d^4y \int d^4z\, e^{ipx-ip'y-iqz}(-1)\mathrm{Tr}V^{aP0n}(x)S(x,y)V^{a'V0n'}_\nu(y)S(y,z)\gamma^\mu \frac{1-\gamma_5}{2} V^{\mathrm{CKM}} S(z,x) \right. \\
&\quad + \int d\sigma_B \int d^4x \int d^4y\, e^{ipx-iqx-ip'y}(-1)\mathrm{Tr}V^{aP0n;\mu}(x;-q)S(x,y)V^{a'V0n'}_\nu(y)S(y,x) \\
&\quad \left. + \int d\sigma_B \int d^4x \int d^4y e^{ipx-ip'x-iqy}(-1)\mathrm{Tr}V^{aP0n}(x)S(x,y)V^{a'V0n';\mu}_\nu(y;-q)S(y,x) \right]
\end{aligned} \tag{19}$$

for vector mesons. Each term is finite, and no regularization is needed. Only the first term in Eq. (19) contributes to the form factor V defined by Eq. (17). Analogously to Eqs. (13) and (14), the first term in the above formulas corresponds to the matrix element

$$\langle H'|q'\gamma^\mu(1-\gamma_5)q|H\rangle.$$

Formulas (18) and (19) allow to extract form factors defined with formulas (16) and (17), and hence phenomenology of semileptonic decays. The differential decay rate is given by

$$\frac{d\Gamma}{dq^2 d\cos\theta} = \frac{p^*}{(2\pi)^3 32M^2}\left(1-\frac{m^2}{q^2}\right)\sum_{\mathrm{pol}}|A|^2.$$

TABLE IV. Decays $P \to P'\ell\bar{\nu}_\ell$ or their charge conjugates. Unless indicated otherwise, the data for comparison are taken from PDG [23]. The width of K_L is the sum of the charge states. The value for $F_0^{K^-\pi^0}$ is found by dividing $F_+^{K^0\pi^-}(0)$ taken from Ref. [32] by $\sqrt{2}$.

	Available data		This work	
Decay	$F_+(0)$	Branching ratio	$F_+(0)$	Branching ratio
$K^- \to \pi^0 e^- \bar{\nu}_e$		$(5.07 \pm 0.04) \times 10^{-2}$	0.699	4.68×10^{-2}
$K^- \to \pi^0 \mu^- \bar{\nu}_\mu$		$(3.352 \pm 0.033) \times 10^{-2}$		3.05×10^{-2}
$K_L \to \pi^\pm e^\mp \nu_e$	0.6856 ± 0.0010 [32]	$(4.055 \pm 0.011) \times 10^{-1}$	0.699	3.86×10^{-1}
$K_L \to \pi^\pm \mu^\mp \nu_\mu$		$(2.704 \pm 0.001) \times 10^{-1}$		2.52×10^{-1}
$D^0 \to K^- e^+ \nu_e$	0.7368 ± 0.0044 [33]	$(3.549 \pm 0.026) \times 10^{-2}$	0.813	3.68×10^{-2}
$D^0 \to K^- \mu^+ \nu_\mu$		$(3.41 \pm 0.04) \times 10^{-2}$		3.57×10^{-2}
$D^0 \to \pi^- e^+ \nu_e$	0.6372 ± 0.0091 [33]	$(2.91 \pm 0.04) \times 10^{-3}$	0.745	2.91×10^{-3}
$D^0 \to \pi^- \mu^+ \nu_\mu$		$(2.67 \pm 0.12) \times 10^{-3}$		2.85×10^{-3}
$D^+ \to \bar{K}^0 e^+ \nu_e$	0.725 ± 0.013 [34]	$(8.72 \pm 0.09) \times 10^{-2}$	0.813	9.27×10^{-2}
$D^+ \to \bar{K}^0 \mu^+ \nu_\mu$		$(8.76 \pm 0.19) \times 10^{-2}$		8.99×10^{-2}
$D^+ \to \pi^0 e^+ \nu_e$	0.440 ± 0.009 [34]	$(3.72 \pm 0.17) \times 10^{-3}$	0.527	3.66×10^{-3}
$D^+ \to \pi^0 \mu^+ \nu_\mu$		$(3.50 \pm 0.15) \times 10^{-3}$		3.59×10^{-3}
$D_s^+ \to K^0 e^+ \nu_e$	0.720 ± 0.085 [35]	$(3.4 \pm 0.4) \times 10^{-3}$	0.611	2.18×10^{-3}
$B^0 \to D^- \ell^+ \nu_\ell$	0.717 ± 0.05 [36]	$(2.24 \pm 0.09) \times 10^{-2}$	0.839	2.99×10^{-2}
$B^0 \to D^- \tau^+ \nu_\tau$		$(1.05 \pm 0.23) \times 10^{-2}$		7.73×10^{-3}
$B^0 \to \pi^- \ell^+ \nu_\ell$	0.297 ± 0.030 [37]	$(1.50 \pm 0.06) \times 10^{-4}$	0.348	1.83×10^{-4}
$B^+ \to \bar{D}^0 \ell \bar{\nu}_\ell$		$(2.30 \pm 0.09) \times 10^{-2}$	0.839	3.23×10^{-2}
$B^+ \to \bar{D}^0 \tau \bar{\nu}_\tau$		$(7.7 \pm 2.5) \times 10^{-3}$		8.33×10^{-3}
$B^+ \to \pi^0 \ell^+ \nu_\ell$		$(7.8 \pm 0.27) \times 10^{-5}$	0.246	9.85×10^{-5}
$B_s^0 \to K^- \mu^+ \nu_\mu$	0.336 ± 0.023 [38]	$(1.06 \pm 0.09) \times 10^{-4}$	0.270	1.34×10^{-4}
$B_s^0 \to D_s^- \mu^+ \nu_\mu$	0.665 ± 0.012 [39]	$(2.44 \pm 0.23) \times 10^{-2}$	0.801	2.87×10^{-2}

Here p^* is the absolute value of final meson momentum in the rest frame of decaying meson

$$p^{*2} = \frac{\left(M^2 - \left(M' - \sqrt{q^2}\right)^2\right)\left(M^2 - \left(M' + \sqrt{q^2}\right)^2\right)}{4M^2},$$

and $\pi - \theta$ is the angle between the momenta of final lepton and final meson in the center of mass of final lepton-neutrino pair $q = (\sqrt{q^2}, 0)$. In this reference frame integration over angle θ is trivial, and one easily finds the total semileptonic decay rate

$$\Gamma = \int_{m^2}^{(M-M')^2} dq^2 \int_{-1}^{1} d\cos\theta \frac{d\Gamma}{dq^2 d\cos\theta}. \qquad (20)$$

The results of calculations are presented in Tables IV and V. Branching ratios are found by dividing decay width (20) by the total decay width taken from Ref. [23]. These tables also contain some parameters of form factors: $F_+(0)$ for final-state pseudoscalar mesons (16), and

$$r_2 = \frac{A_2(0)}{A_1(0)}, \qquad r_V = \frac{V(0)}{A_1(0)}$$

for vector meson in the final state (17).

The isospin symmetry $m_u = m_d$ in the present framework is exact, so the following relations for calculated form factors of semileptonic decays hold:

TABLE V. Decays $P \to V\ell\bar{\nu}_\ell$ or their charge conjugates. The data for comparison are taken from PDG [23] if not indicated otherwise.

	Available data			This work		
Decay	r_V	r_2	Branching ratio	r_V	r_2	Branching ratio
$D^0 \to \rho^- e^+ \nu_e$	1.64 ± 0.10	0.84 ± 0.06	$(1.50 \pm 0.12) \times 10^{-3}$	1.37	0.819	3.35×10^{-3}
$D^0 \to \rho^- \mu^+ \nu_\mu$			$(1.35 \pm 0.13) \times 10^{-3}$			3.20×10^{-3}
$D^0 \to K^{*-} e^+ \nu_e$	1.46 ± 0.07	0.68 ± 0.06	$(2.15 \pm 0.16) \times 10^{-2}$	1.24	0.788	4.07×10^{-2}
$D^0 \to K^{*-} \mu^+ \nu_\mu$			$(1.89 \pm 0.24) \times 10^{-2}$			3.84×10^{-2}
$D^+ \to \rho^0 e^+ \nu_e$	1.64 ± 0.10	0.84 ± 0.06	$(2.18\,^{+0.17}_{-0.25}) \times 10^{-3}$	1.37	0.819	4.22×10^{-3}
$D^+ \to \rho^0 \mu^+ \nu_\mu$			$(2.4 \pm 0.4) \times 10^{-3}$			4.03×10^{-3}
$D^+ \to \omega e^+ \nu_e$	1.24 ± 0.11	1.06 ± 0.16	$(1.69 \pm 0.11) \times 10^{-3}$	1.37	0.819	4.22×10^{-3}
$D^+ \to \omega \mu^+ \nu_\mu$			$(1.77 \pm 0.21) \times 10^{-3}$			4.03×10^{-3}
$D^+ \to \bar{K}^{*0} e^+ \nu_e$	1.49 ± 0.05	0.802 ± 0.021	$(5.40 \pm 0.10) \times 10^{-2}$	1.24	0.788	1.02×10^{-1}
$D^+ \to \bar{K}^{*0} \mu^+ \nu_\mu$			$(5.27 \pm 0.15) \times 10^{-2}$			9.66×10^{-2}
$D_s^+ \to \phi e^+ \nu_e$	1.80 ± 0.08	0.84 ± 0.11	$(2.39 \pm 0.16) \times 10^{-2}$	1.36	0.879	3.54×10^{-2}
$D_s^+ \to \phi \mu^+ \nu_\mu$			$(1.9 \pm 0.5) \times 10^{-2}$			3.34×10^{-2}
$D_s^+ \to K^{*0} e^+ \nu_e$	1.7 ± 0.4	0.77 ± 0.29	$(2.15 \pm 0.28) \times 10^{-3}$	1.46	0.689	2.82×10^{-3}
$B^0 \to \rho^- \ell^+ \nu_\ell$	1.270 ± 0.240 [40]	0.874 ± 0.192 [40]	$(2.94 \pm 0.21) \times 10^{-4}$	1.17	0.928	8.14×10^{-4}
$B^0 \to D^{*-} \ell^+ \nu_\ell$	1.151 ± 0.114 [40]	0.856 ± 0.076 [40]	$(4.97 \pm 0.12) \times 10^{-2}$	1.06	0.926	6.82×10^{-2}
$B^0 \to D^{*-} \tau^+ \nu_\tau$			$(1.58 \pm 0.09) \times 10^{-2}$			1.47×10^{-2}
$B^+ \to \rho^0 \ell^+ \nu_\ell$			$(1.58 \pm 0.44) \times 10^{-4}$	1.17	0.928	4.39×10^{-4}
$B^+ \to \omega \ell^+ \nu_\ell$	1.254 ± 0.056 [41]	0.878 ± 0.081 [41]	$(1.19 \pm 0.09) \times 10^{-4}$	1.17	0.928	4.39×10^{-4}
$B^+ \to \bar{D}^{*0} \ell^+ \nu_\ell$			$(5.58 \pm 0.22) \times 10^{-2}$	1.06	0.926	7.36×10^{-2}
$B^+ \to \bar{D}^{*0} \tau^+ \nu_\tau$			$(1.88 \pm 0.20) \times 10^{-2}$			1.58×10^{-2}
$B_s^0 \to D_s^{*-} \mu^+ \nu_\mu$	1.64 ± 0.278 [42]	0.958 ± 0.146 [42]	$(5.3 \pm 0.5) \times 10^{-2}$	1.10	0.959	5.75×10^{-2}

$$F_\pm^{D^0\to\pi^-} = \sqrt{2} F_\pm^{D^+\to\pi^0}, \qquad F_i^{D^0\to\rho^-} = \sqrt{2} F_i^{D^+\to\rho^0} = \sqrt{2} F_i^{D^+\to\omega},$$
$$F_\pm^{D^0\to K^-} = F_\pm^{D^+\to\bar{K}^0}, \qquad F_i^{D^0\to K^{*-}} = F_i^{D^+\to\bar{K}^{*0}},$$
$$F_\pm^{B^0\to\pi^-} = \sqrt{2} F_\pm^{B^+\to\pi^0}, \qquad F_i^{B^0\to\rho^-} = \sqrt{2} F_i^{B^+\to\rho^0} = \sqrt{2} F_i^{B^+\to\omega},$$
$$F_\pm^{B^0\to D^-} = F_\pm^{B^+\to D^0}, \qquad F_i^{B^0\to D^{*-}} = F_i^{B^+\to D^{*0}},$$

where $F_i = A_0, A_1, A_2, V$. For the purposes of the present paper it also suffices to neglect CP-violation, so additionally

$$F_\pm^{K^-\to\pi^0} = F_\pm^{K_L\to\pi^+} = F_\pm^{K_L\to\pi^-}.$$

The vertex (8), and consequently (11), results from the expansion of a bilocal quark current in terms of basis functions around its "center of mass" [6]. The vertex with W boson (11) changes quark flavor and hence mass, and this might lead to exponential growth of individual terms in the sum over radial number n in formulas (18) and (19), which is typical of nonlocal theories. The sums over n then appear as a result of large number cancellation which makes them difficult to evaluate numerically. Among the considered semileptonic decays, this happens with the decays of D_s into K, K^*, B into π, ρ, ω, and B_s into K. The impulse approximation is unaffected by this numerical instability, while additional "nonlocal" contributions are neglected for these decays as they are expected to be smaller. The latter is mentioned in Ref. [43] and can be observed in semileptonic decays where there is no numerical instability.

TABLE VI. Parameters of double-pole parametrization (22) fitted to form factors of $P \to P'\ell\bar{\nu}_\ell$ extracted from the amplitude (18). Rows with label "full" include all terms in Eq. (18), while in "imp. approx." only the term corresponding to the impulse approximation is retained.

		F_+			F_-		
		$F_+(0)$	a	b	$F_-(0)$	a	b
$K^- \to \pi^0\ell\bar{\nu}_\ell$	Full	0.699	0.279	0.00537	−0.0964	0.210	0.00703
	Imp. approx.	0.697	0.280	0.00606	−0.0876	0.224	0.00962
$D^0 \to \pi^-\overline{\ell}\nu_\ell$	Full	0.745	0.657	−0.0364	−0.375	0.813	0.0830
	Imp. approx.	0.648	0.772	0.0490	−0.382	0.790	0.0641
$D^0 \to K^-\overline{\ell}\nu_\ell$	Full	0.813	0.614	0.0137	−0.388	0.642	0.0282
	Imp. approx.	0.803	0.624	0.0205	−0.386	0.644	0.0287
$D_s \to K^0\overline{\ell}\nu_\ell$	Imp. approx.	0.611	1.02	0.185	−0.388	1.05	0.197
$B^0 \to \pi^-\overline{\ell}\nu_\ell$	Imp. approx.	0.348	1.08	0.170	−0.285	1.09	0.181
$B_s^0 \to K^-\overline{\ell}\nu_\ell$	Imp. approx.	0.270	1.39	0.434	−0.230	1.40	0.434
$B^0 \to D^-\overline{\ell}\nu_\ell$	Full	0.839	0.629	0.0227	−0.382	0.635	0.0237
	Imp. approx.	0.840	0.629	0.0231	−0.382	0.635	0.0233
$B_s^0 \to D_s^-\overline{\ell}\nu_\ell$	Full	0.801	0.807	0.115	−0.360	0.840	0.142
	Imp. approx.	0.785	0.828	0.135	−0.363	0.832	0.135

One notices that the branching ratios of semileptonic decays with light final-state vector mesons such as $D^0 \to \rho^- e^+ \nu_e$ (see Table V) are in poor agreement with experimental data. However, the experimental values given in Table V are not measured directly, but rather extracted from semileptonic decays with a couple of final-state pseudoscalar mesons

$$P \to P'P''\ell\nu_\ell. \tag{21}$$

In doing so, these decays are considered to take place via resonances and the Breit-Wigner function is employed for the description of their shape (see e.g. Ref. [44]). In the domain model, the meson propagator (3) resembles the free particle propagator only in the vicinity of the meson pole. If one includes finite width in propagator (1), it is expected to be adequately approximated by Breit-Wigner form only for narrow resonances. Assumedly, this is why decay width for $B^0_{(s)} \to D^{*-}_{(s)}\mu^+\nu_\mu$ is in much better

TABLE VII. Parameters of double-pole parametrization (22) fitted to form factors of $P \to V\ell\bar{\nu}_\ell$ extracted from the amplitude (19). Rows with label "full" include all terms in Eq. (19), while in "imp. approx." only the term corresponding to the impulse approximation is retained.

		A_0			A_1			A_2			V		
		$A_0(0)$	a	b	$A_1(0)$	a	b	$A_2(0)$	a	b	$V(0)$	a	b
$D^0 \to \rho^-\overline{\ell}\nu_\ell$	Full	1.07	0.972	0.248	0.948	0.113	0.0258	0.777	0.316	0.196	1.30	0.785	0.0908
	Imp. approx.	1.14	0.894	0.168	0.953	0.110	0.0249	0.688	0.370	0.237	1.30	0.785	0.0908
$D^0 \to K^{*-}\overline{\ell}\nu_\ell$	Full	1.03	0.779	0.130	0.922	0.118	−0.00706	0.726	0.433	0.0543	1.14	0.683	0.0613
	Imp. approx.	1.03	0.762	0.112	0.921	0.118	−0.00715	0.715	0.441	0.0584	1.14	0.683	0.0613
$D_s \to \phi\overline{\ell}\nu_\ell$	Full	0.856	1.08	0.352	0.811	0.349	−0.00735	0.713	0.569	0.0943	1.10	0.936	0.191
	Imp. approx.	0.889	1.00	0.256	0.809	0.347	−0.00883	0.633	0.645	0.154	1.10	0.936	0.191
$D_s^+ \to K^{*0}\overline{\ell}\nu_\ell$	Imp. approx.	0.855	1.18	0.361	0.719	0.397	0.00367	0.495	0.580	0.343	1.05	1.09	0.267
$B^0 \to \rho^-\overline{\ell}\nu_\ell$	Imp. approx.	0.670	1.30	0.373	0.559	0.294	0.00389	0.519	1.02	0.296	0.656	1.18	0.265
$B^0 \to D^{*-}\overline{\ell}\nu_\ell$	Full	0.891	0.769	0.110	0.843	0.190	−0.0316	0.780	0.679	0.0733	0.890	0.733	0.0817
	Imp. approx.	0.893	0.762	0.103	0.844	0.190	−0.0316	0.780	0.680	0.0738	0.890	0.733	0.0817
$B_s^0 \to D_s^-\overline{\ell}\nu_\ell$	Full	0.788	1.03	0.278	0.766	0.414	−0.0237	0.734	0.871	0.160	0.843	0.957	0.204
	Imp. approx.	0.805	0.989	0.235	0.768	0.412	−0.0246	0.716	0.894	0.182	0.843	0.957	0.204

agreement with experiment (see Table V) because the widths of D^* and D_s^* are relatively small. Another source of uncertainty is nonresonant contribution to the decay (21) which would interfere with the resonant one. Overall, the comparison of model result with experimental data for four-body decay (21) would be more conclusive, but this requires evaluation of both resonant and nonresonant contributions, which is beyond the scope of the present paper. The ratios r_2, r_V are not sensitive to the total decay width.

In order to conveniently represent the calculated form factors, they are fitted with the double-pole parametrization

$$F_i = F_i(0)\left[1 - a\frac{q^2}{M_P^2} + b\left(\frac{q^2}{M_P^2}\right)^2\right]^{-1} \tag{22}$$

in the physical region of q^2. The results of the fits are given in Tables VI and VII, and the fitting error is negligible for the present framework. The Tables VI and VII allow to compare the contribution of all diagrams in Fig. 3 with the impulse approximation where the former is accessible.

V. SUMMARY AND OUTLOOK

The domain model of QCD vacuum and hadronization is a mean-field approach that allows unified description of basic low-energy properties of QCD and meson physics. In the present work, the model was applied to the leptonic and semileptonic decays of mesons. The numerical results for leptonic decay constants, semileptonic form factors and branching ratios are presented. The phenomenological description is reasonable with the exception of branching ratios $\mathcal{B}(P \to V\ell\bar{\nu}_\ell)$ for large-width mesons V.

When one consistently introduces the electroweak interactions into the model, the corresponding amplitudes of these decays get contributions due to vertices in Fig. 1 in addition to the impulse approximation. Among the decays considered in the present paper, the vertices in Fig. 1 give the most prominent numerical contribution to the leptonic decays of pseudoscalar mesons (Table II), while the effect on semileptonic decays is much smaller numerically, with the exception of $D \to \pi$ and $D \to \rho$ (Tables VI and VII). The impulse approximation for leptonic decays of vector mesons in not even meaningful on its own. The domain model is obviously an effective model with limited precision, but the findings of the present work indicate that vertices in Fig. 1 should be taken into account when extracting CKM matrix from the experimental data. It is plausible that the tension between determination of CKM matrix elements from inclusive and exclusive semileptonic decays, leptonic decays and semileptonic decays can be related to contributions in Fig. 1, as well as deviation from unitarity of CKM matrix (see, e.g., review [4]).

TABLE VIII. The central value for ratio (25) calculated from experimental data [Eqs. (23) and (24)], Lattice QCD (Ref. [2], Eq. (178) and Ref. [4], Table 291) and Tables II and VI. The closer this ratio to the experimental value, the more consistent thus extracted elements $|V_{cs}|$ would be.

$\frac{\lvert V_{cs}\rvert f_{D_s}}{\lvert V_{cs}\rvert F_+^{D\to K}(0)}$, MeV		$\frac{f_{D_s}}{F_+^{D\to K}(0)}$, MeV	
Experimental	LQCD	Imp. approx.	Full
341.8	328.8	305.9	352.8

For example, consider the tension in the values of $|V_{cs}|$ extracted from leptonic or semileptonic decays with Lattice QCD, which is reported to be $\sim 2\sigma$ (see Ref. [4], Sec. XI.B.3 and Ref. [2], Sec. 7.5). One may find the product [Ref. [4], Eq. (316)]

$$|V_{cs}| f_{D_s} = (245.4 \pm 2.4)\ \text{MeV} \tag{23}$$

from experimentally measured branching ratios of leptonic decays of D_s, masses of D_s and leptons, and D_s lifetime. Now, if one uses either the "imp. approx." or "full" values for f_{D_S} in Table II, the extracted central values of $|V_{cs}|$ would differ by approximately 15%. At the same time, the values of $|V_{cs}|$ extracted from the world average of experimentally measured value (Ref. [4], Table 288)

$$|V_{cs}| F_+^{D\to K}(0) = 0.7180(33) \tag{24}$$

and either the "imp. approx." or "full" values of $F_+^{D\to K}(0)$ in Table VI would differ by 1%. It is more illuminating to consider the ratio

$$\frac{|V_{cs}| f_{D_s}}{|V_{cs}| F_+^{D\to K}(0)} = \frac{f_{D_s}}{F_+^{D\to K}(0)} \tag{25}$$

which is given in Table VIII for several cases. The contribution of diagrams in Fig. 1 brings the ratio (25) closer to the experimental value and hence improves the description of meson dynamics within the model and decreases the tension between the values of $|V_{cs}|$ extracted from leptonic or semileptonic decays. The overall effect, however, is comparable with the precision of the model. The actual extraction of CKM matrix elements with proper assessment of uncertainties and standard model constraints

FIG. 4. Additional diagrams contributing to the amplitude of $P \to \eta^{(\prime)}\ell\bar{\nu}_\ell$ in the domain model. The dark gray denotes correlation of quark loops by the vacuum field analogous to the second term in Eq. (4).

is based on the most precise available data, both experimentally and theoretically, see Refs. [45–48] and minireview in PDG (Section 12 in Ref. [23]).

The decays involving η and η' mesons were not considered in the present work because there are additional contributions to corresponding amplitudes. The diagrams for these contributions are shown in Fig. 4, their origin is analogous to the second term of Eq. (4). These decays require a separate thorough analysis and will be considered elsewhere.

ACKNOWLEDGMENTS

The author is grateful to Sergei Nedelko for fruitful and stimulating discussions.

APPENDIX: VERTEX FUNCTION

$$\begin{aligned} F_{nl}(s) &= s^n \int_0^1 dt t^{n+l} \exp(st) = \int_0^1 dt t^{n+l} \frac{\partial^n}{\partial t^n} \exp(st) \\ &= t^{n+l} \frac{\partial^{n-1}}{\partial t^{n-1}} \exp(st)\Big|_{t=0}^1 - \int_0^1 dt (n+l) t^{n-1+l} \frac{\partial^{n-1}}{\partial t^{n-1}} \exp(st) = \ldots \\ &= (-1)^n (n+l)! \left[\sum_{m=1}^{n} (-1)^m \frac{1}{(m+l)!} s^{m-1} \exp(s) + \frac{1}{l!} \int_0^1 dt t^l \exp(st) \right]. \end{aligned} \tag{A1}$$

The terms s^n containing kinematic variables make formulas significantly larger. In order to avoid this difficulty, formula (A1) for vertex function F_{nl} can be transformed further with the help of the identity

$$s^n = \frac{n!}{2\pi i} \oint_\Gamma \frac{dz}{z^{n+1}} \exp sz, \quad n = 0, 1, 2, \ldots \tag{A2}$$

where the closed contour Γ encircles zero. After substituting Eq. (A2) into Eq. (A1) and using several identities one finds

$$\begin{aligned} F_{nl} &= (-1)^n (n+l)! \int_0^1 dt \Bigg[\exp(s(r\exp(i2\pi t) + 1)) \\ &\quad \times \left\{ \sum_{m=2}^{n} \frac{(-1)^m}{(m+l)!} \frac{(m-1)!}{r^{m-1}} \exp(i2\pi(1-m)t) \right\} - \frac{\exp s}{(l+1)!} + \frac{t^l}{l!} \exp(st) \Bigg] \\ &= (-1)^n (n+l)! \int_0^1 dt \Bigg[\frac{t^l}{l!} \exp(st) - \frac{\exp s}{(l+1)!} + \sum_{m=2}^{n} \frac{(-1)^m}{(m+l)!} \frac{(m-1)!}{r^{m-1}} \frac{-i}{m-1} \\ &\quad \times \sum_{j=0}^{m-2} \{ \exp[sf(t/2 - j, m, r)] - \exp[sf(-t/2 + j, m, r)] \} \sin \pi t \Bigg] \end{aligned}$$

where

$$f(t, m, r) = r \exp\left(i2\pi \frac{t}{m-1} \right) + 1$$

and $0 < r \leq 1$ is an arbitrary parameter.

[1] R. J. Hill, The modern description of semileptonic meson form factors, eConf **C060409**, 027 (2006), https://www.slac.stanford.edu/econf/C060409/papers/fpcp2006_RichardHill.pdf.

[2] Y. Aoki *et al.* (Flavour Lattice Averaging Group (FLAG)), FLAG review 2021, Eur. Phys. J. C **82**, 869 (2022).

[3] J. D. Richman and P. R. Burchat, Leptonic and semileptonic decays of charm and bottom hadrons, Rev. Mod. Phys. **67**, 893 (1995).

[4] Y. S. Amhis *et al.* (HFLAV Collaboration), Averages of b-hadron, c-hadron, and τ-lepton properties as of 2021, Phys. Rev. D **107**, 052008 (2023).

[5] M. A. Ivanov, Y. L. Kalinovsky, and C. D. Roberts, Survey of heavy meson observables, Phys. Rev. D **60**, 034018 (1999).

[6] G. V. Efimov and S. N. Nedelko, Nambu–Jona-Lasinio model with the homogeneous background gluon field, Phys. Rev. D **51**, 176 (1995).

[7] J. V. Burdanov, G. V. Efimov, S. N. Nedelko, and S. A. Solunin, Meson masses within the model of induced nonlocal quark currents, Phys. Rev. D **54**, 4483 (1996).

[8] A. C. Kalloniatis and S. N. Nedelko, Realization of chiral symmetry in the domain model of QCD, Phys. Rev. D **69**, 074029 (2004); **70**, 119903(E) (2004).

[9] S. N. Nedelko and V. E. Voronin, Regge spectra of excited mesons, harmonic confinement and QCD vacuum structure, Phys. Rev. D **93**, 094010 (2016).

[10] S. N. Nedelko and V. E. Voronin, Influence of confining gluon configurations on the $P \to \gamma^* \gamma$ transition form factors, Phys. Rev. D **95**, 074038 (2017).

[11] S. N. Nedelko and V. E. Voronin, Domain wall network as QCD vacuum and the chromomagnetic trap formation under extreme conditions, Eur. Phys. J. A **51**, 45 (2015).

[12] S. N. Nedelko and V. E. Voronin, Energy-driven disorder in mean field QCD, Phys. Rev. D **103**, 114021 (2021).

[13] A. C. Kalloniatis and S. N. Nedelko, Confinement and chiral symmetry breaking via domainlike structures in the QCD vacuum, Phys. Rev. D **64**, 114025 (2001).

[14] S. Nedelko and V. Voronin, Dipole polarizabilities of light pseudoscalar mesons within the domain model of the QCD vacuum, Phys. Rev. D **107**, 094027 (2023).

[15] S. Nedelko, A. Nikolskii, and V. Voronin, Soft gluon fields and anomalous magnetic moment of muon, J. Phys. G **49**, 035003 (2022).

[16] M. A. Ivanov, J. G. Körner, J. N. Pandya, P. Santorelli, N. R. Soni, and C.-T. Tran, Exclusive semileptonic decays of D and D_s mesons in the covariant confining quark model, Front. Phys. (Beijing) **14**, 64401 (2019).

[17] S. Dubnička, A. Z. Dubničková, M. A. Ivanov, and A. Liptaj, B meson decays in the covariant confined quark model, Symmetry **15**, 1542 (2023).

[18] J. Terning, Gauging nonlocal Lagrangians, Phys. Rev. D **44**, 887 (1991).

[19] F. Gross and D. O. Riska, Current conservation and interaction currents in relativistic meson theories, Phys. Rev. C **36**, 1928 (1987).

[20] R. M. Woloshyn, Relativistic effects in bound-state form factors, Phys. Rev. C **12**, 901 (1975).

[21] W. Bentz, Two-body Ward identities, Nucl. Phys. **A446**, 678 (1985).

[22] J. Kuipers, T. Ueda, J. A. M. Vermaseren, and J. Vollinga, FORM version 4.0, Comput. Phys. Commun. **184**, 1453 (2013).

[23] R. L. Workman *et al.* (Particle Data Group), Review of particle physics, Prog. Theor. Exp. Phys. **2022**, 083C01 (2022).

[24] R. J. Dowdall, C. T. H. Davies, T. C. Hammant, and R. R. Horgan, Precise heavy-light meson masses and hyperfine splittings from lattice QCD including charm quarks in the sea, Phys. Rev. D **86**, 094510 (2012).

[25] A. Bazavov, C. Bernard, N. Brown, C. DeTar, A. X. El-Khadra, E. Gámiz, S. Gottlieb, U. M. Heller, J. Komijani, A. S. Kronfeld, J. Laiho, P. B. Mackenzie, E. T. Neil, J. N. Simone, R. L. Sugar, D. Toussaint, and R. S. Van de Water, B- and D-meson leptonic decay constants from four-flavor lattice QCD, Phys. Rev. D **98**, 074512 (2018).

[26] C. McNeile, C. T. H. Davies, E. Follana, K. Hornbostel, and G. P. Lepage, Heavy meson masses and decay constants from relativistic heavy quarks in full lattice QCD, Phys. Rev. D **86**, 074503 (2012).

[27] W. Sun, A. Alexandru, Y. Chen, T. Draper, Z. Liu, and Y.-B. Yang (χQCD Collaboration), Anatomy of the ρ resonance from lattice QCD at the physical point, Chin. Phys. C **42**, 063102 (2018).

[28] G. C. Donald, C. T. H. Davies, J. Koponen, and G. P. Lepage (HPQCD Collaboration), V_{cs} from $D_s \to \phi \ell \nu$ semileptonic decay and full lattice QCD, Phys. Rev. D **90**, 074506 (2014).

[29] V. Lubicz, A. Melis, and S. Simula (ETM Collaboration), Masses and decay constants of $D^*_{(s)}$ and $B^*_{(s)}$ mesons with $N_f = 2 + 1 + 1$ twisted mass fermions, Phys. Rev. D **96**, 034524 (2017).

[30] B. Colquhoun, C. T. H. Davies, R. J. Dowdall, J. Kettle, J. Koponen, G. P. Lepage, and A. T. Lytle (HPQCD Collaboration), B-meson decay constants: A more complete picture from full lattice QCD, Phys. Rev. D **91**, 114509 (2015).

[31] M. Wirbel, B. Stech, and M. Bauer, Exclusive semileptonic decays of heavy mesons, Z. Phys. C **29**, 637 (1985).

[32] A. Bazavov *et al.* (Fermilab Lattice and MILC Collaborations), $|V_{us}|$ from $K_{\ell 3}$ decay and four-flavor lattice QCD, Phys. Rev. D **99**, 114509 (2019).

[33] M. Ablikim *et al.* (BESIII Collaboration), Study of dynamics of $D^0 \to K^- e^+ \nu_e$ and $D^0 \to \pi^- e^+ \nu_e$ decays, Phys. Rev. D **92**, 072012 (2015).

[34] M. Ablikim *et al.* (BESIII Collaboration), Analysis of $D^+ \to \bar{K}^0 e^+ \nu_e$ and $D^+ \to \pi^0 e^+ \nu_e$ semileptonic decays, Phys. Rev. D **96**, 012002 (2017).

[35] M. Ablikim *et al.* (BESIII Collaboration), First measurement of the form factors in $D_s^+ \to K^0 e^+ \nu_e$ and $D_s^+ \to K^{*0} e^+ \nu_e$ decays, Phys. Rev. Lett. **122**, 061801 (2019).

[36] J. A. Bailey *et al.* (MILC Collaboration), $B \to D \ell \nu$ form factors at nonzero recoil and $|V_{cb}|$ from $2 + 1$-flavor lattice QCD, Phys. Rev. D **92**, 034506 (2015).

[37] D. Leljak, B. Melić, and D. van Dyk, The $\bar{B} \to \pi$ form factors from QCD and their impact on $|V_{ub}|$, J. High Energy Phys. 07 (2021) 036.

[38] A. Khodjamirian and A. V. Rusov, $B_s \to K\ell\nu_\ell$ and $B_{(s)} \to \pi(K)\ell^+\ell^-$ decays at large recoil and CKM matrix elements, J. High Energy Phys. 08 (2017) 112.
[39] E. McLean, C. T. H. Davies, J. Koponen, and A. T. Lytle, $B_s \to D_s\ell\nu$ form factors for the full q^2 range from lattice QCD with non-perturbatively normalized currents, Phys. Rev. D **101**, 074513 (2020).
[40] N. Gubernari, A. Kokulu, and D. van Dyk, $B \to P$ and $B \to V$ form factors from B-meson light-cone sum rules beyond Leading twist, J. High Energy Phys. 01 (2019) 150.
[41] A. Bharucha, D. M. Straub, and R. Zwicky, $B \to V\ell^+\ell^-$ in the standard model from light-cone sum rules, J. High Energy Phys. 08 (2016) 098.
[42] J. Harrison and C. T. H. Davies (HPQCD Collaboration), $B_s \to D_s^*$ form factors for the full q^2 range from lattice QCD, Phys. Rev. D **105**, 094506 (2022).
[43] A. Faessler, T. Gutsche, B. R. Holstein, M. A. Ivanov, J. G. Körner, and V. E. Lyubovitskij, Semileptonic decays of the light $J^P = 1/2^+$ ground state baryon octet, Phys. Rev. D **78**, 094005 (2008).
[44] S. Dobbs *et al.* (CLEO Collaboration), First measurement of the form factors in the decays $D^0 \to \rho^- e^+ \nu_e$ and $D^+ \to \rho^0 e^+ \nu_e$, Phys. Rev. Lett. **110**, 131802 (2013).
[45] J. Charles, A. Hocker, H. Lacker, S. Laplace, F. R. Le Diberder, J. Malcles, J. Ocariz, M. Pivk, and L. Roos (CKMfitter Group), *CP* violation and the CKM matrix: Assessing the impact of the asymmetric B factories, Eur. Phys. J. C **41**, 1 (2005).
[46] L. Vale Silva, 2023 update of the extraction of the CKM matrix elements, arXiv:2405.08046.
[47] M. Ciuchini, G. D'Agostini, E. Franco, V. Lubicz, G. Martinelli, F. Parodi, P. Roudeau, and A. Stocchi, 2000 CKM triangle analysis: A critical review with updated experimental inputs and theoretical parameters, J. High Energy Phys. 07 (2001) 013.
[48] M. Bona *et al.* (UTfit Collaboration), New UTfit analysis of the unitarity triangle in the Cabibbo-Kobayashi-Maskawa scheme, Rend. Lincei Sci. Fis. Nat. **34**, 37 (2023).